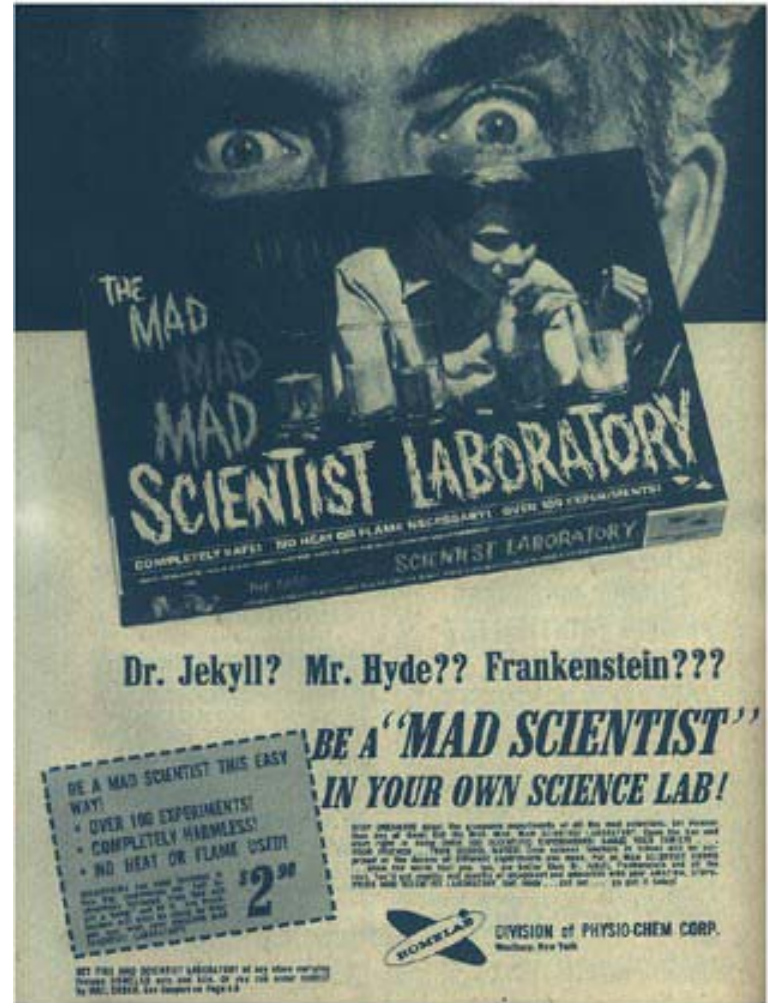

Film Characterization Tutorial

G.J. Mankey, 01/23/04



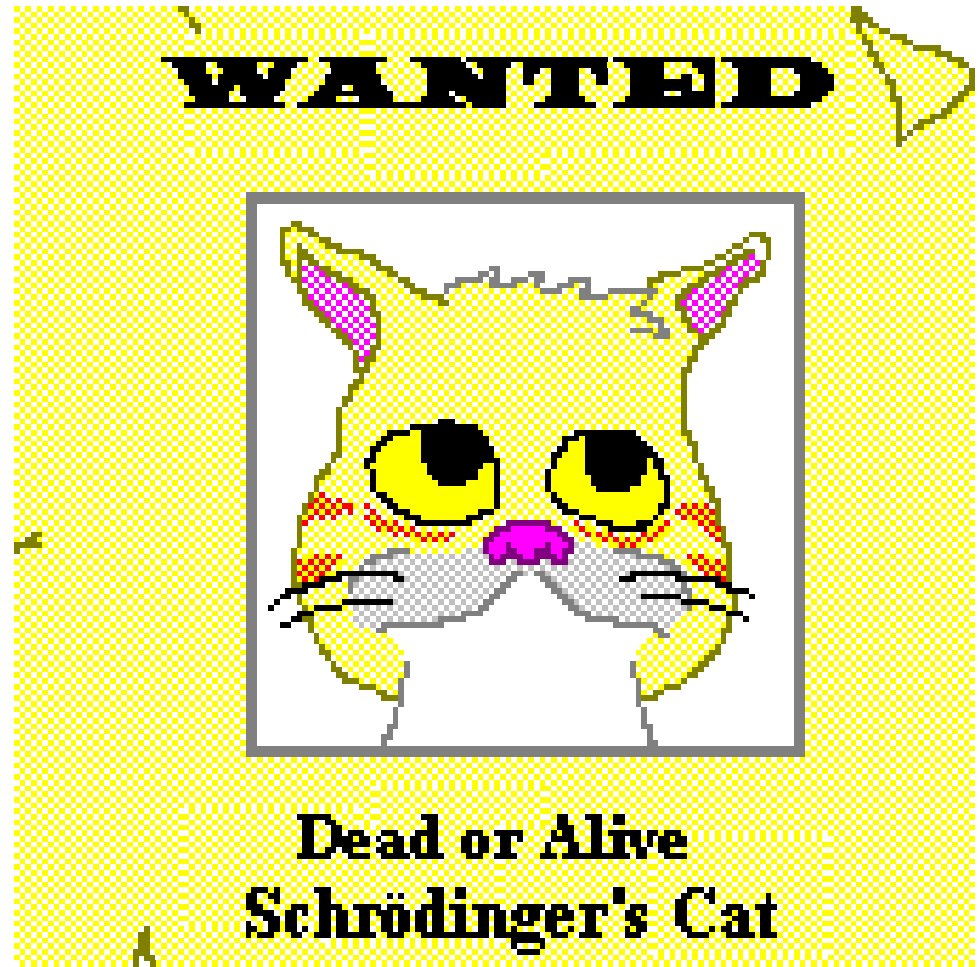
Theory vs. Experiment

- A theory is something nobody believes, except the person who made it. An experiment is something everybody believes, except the person who made it.
 - Albert Einstein

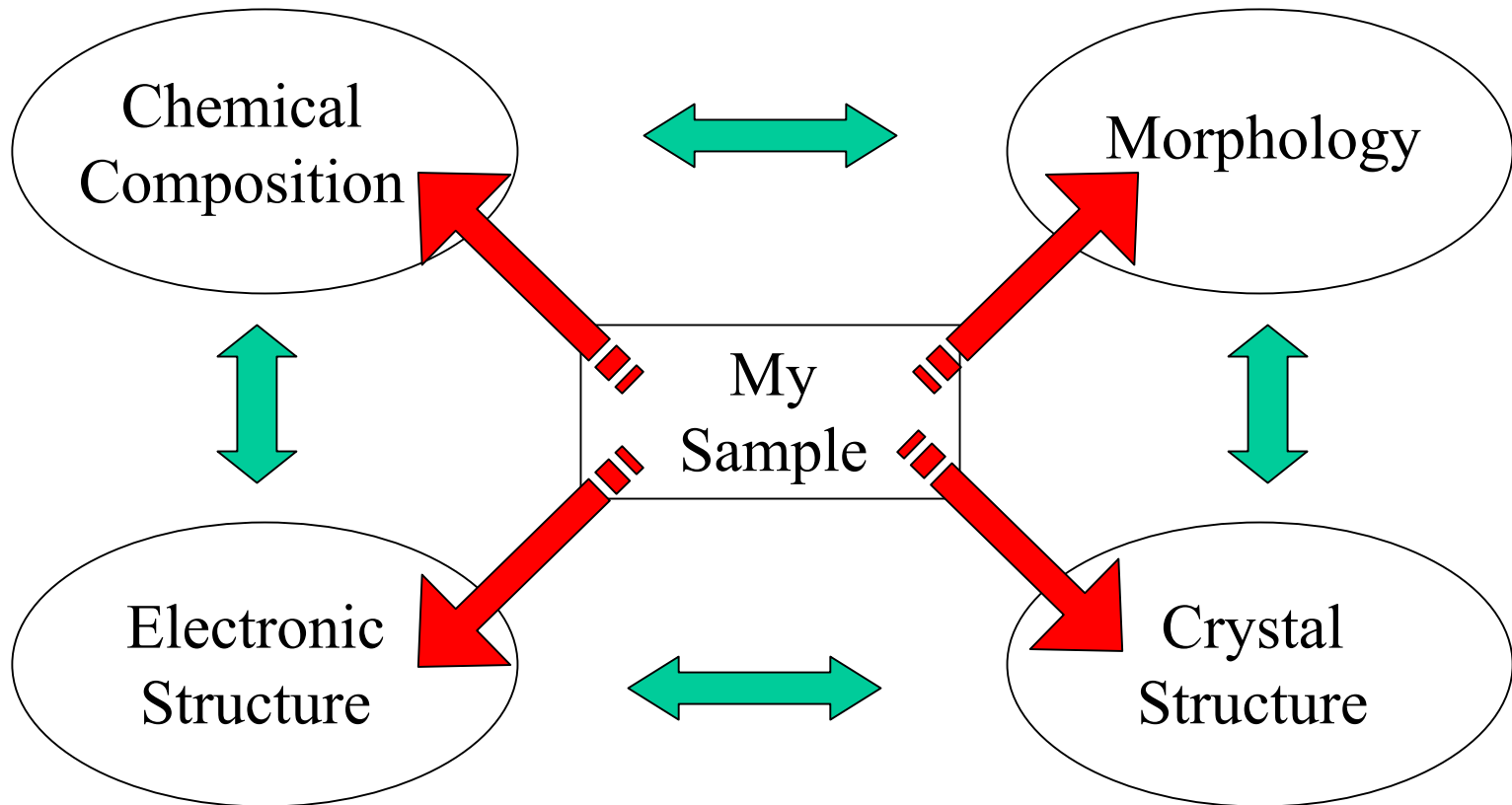


Measurement Techniques

- You won't know the result until you open the box that contains the cat.
- Only the correct measurement will answer your question.



What Property Do You Wish to Know?

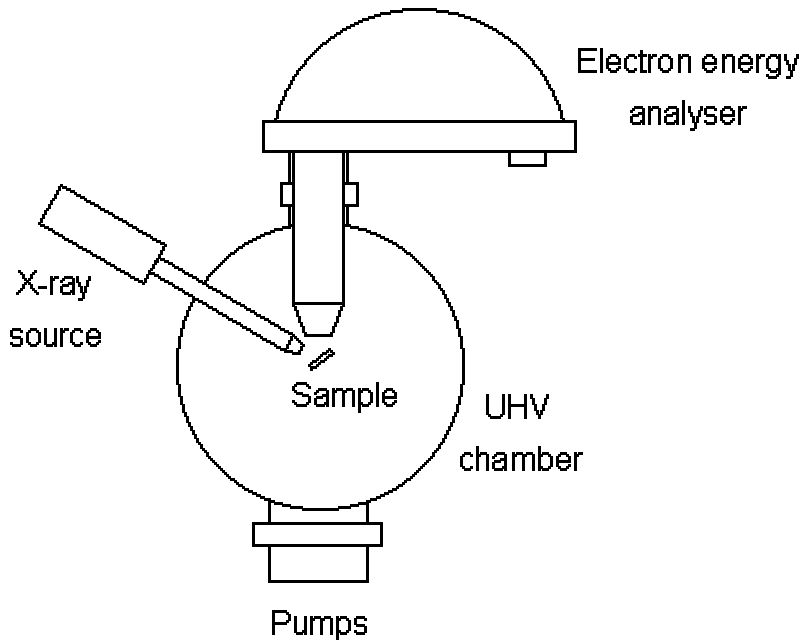


Techniques

- Chemical composition
 - X ray photoelectron spectroscopy (XPS)
 - Auger electron spectroscopy (AES)
 - Energy dispersive analysis of x-rays (EDAX)*
- Electronic structure
 - XPS and UPS*
 - Variable angle spectroscopic ellipsometry (VASE)
- Crystal structure
 - X ray diffraction (XRD)
 - Electron diffraction (LEED and RHEED)*
- Morphology
 - Atomic force microscopy (AFM)
 - Scanning electron microscopy (SEM)*

* Maybe next time

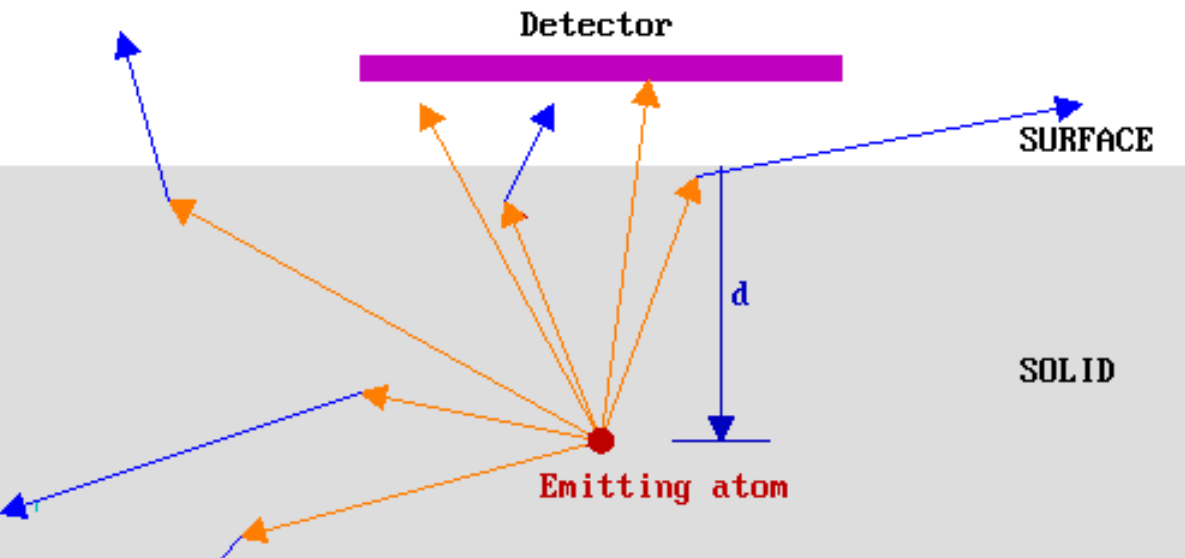
XPS



- The kinetic energies of electrons ejected from the surface of the sample is analyzed with a hemispherical energy analyzer.
- The experiment must be performed in a good vacuum.

Ref: <http://www.chem.qmw.ac.uk/surfaces/scc/>

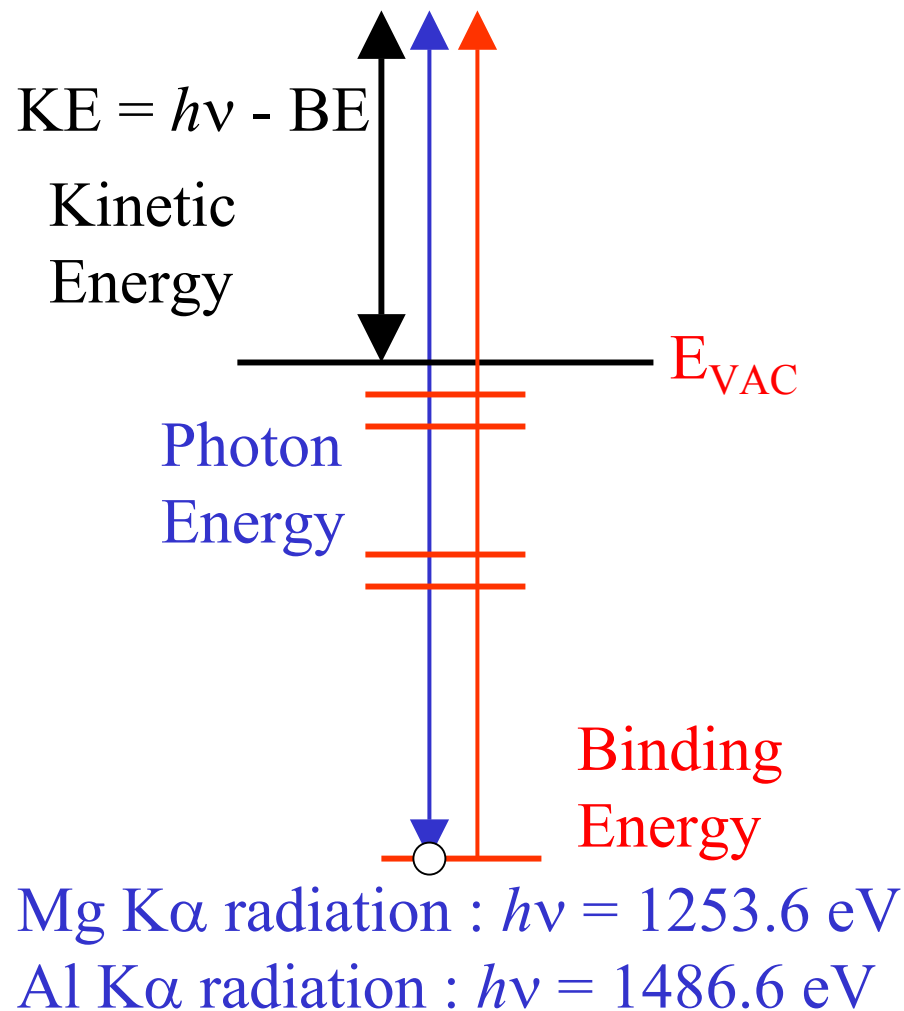
Surface Sensitivity



- The photoelectrons must reach the surface without losing energy to be detected by the spectrometer.
- The probing depth of the experiment is on the nanometer scale.

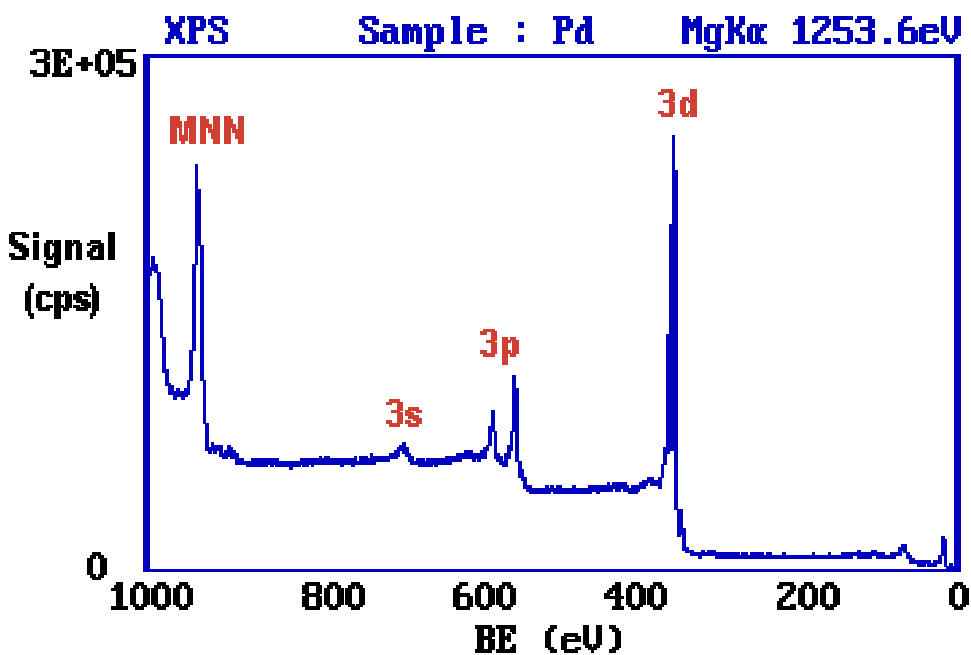
Ref: <http://www.chem.qmw.ac.uk/surfaces/scc/>

Energy Levels in XPS



- The electron spectrometer measures the kinetic energies of ejected electrons.
- Since the x ray source is monochromatic, the binding energies can be found.
- The binding energy is a unique chemical property, so the number of electrons detected at a particular binding energy is proportional to the atomic concentration.

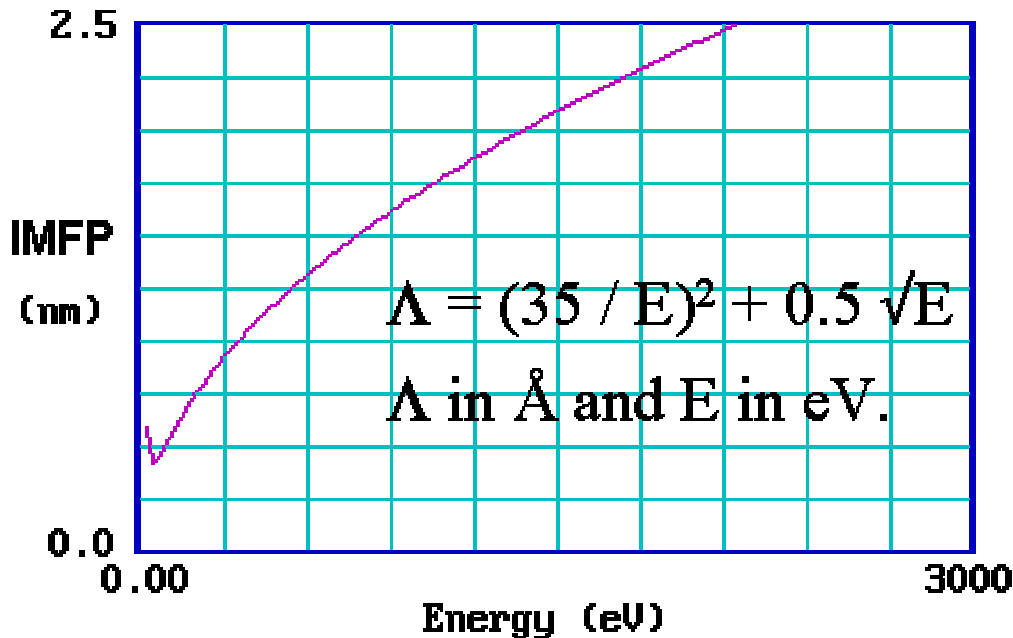
A Typical XPS Spectrum



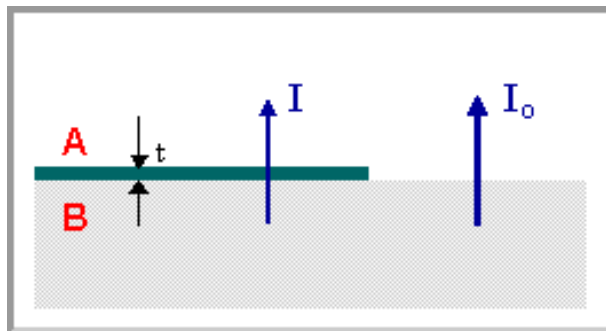
- Working downwards from the highest energy levels
- the valence band ($4d,5s$) emission occurs at a binding energy of ca. 0 - 8 eV (measured with respect to the Fermi level, or alternatively at ca. 4 - 12 eV if measured with respect to the vacuum level).
- the emission from the $4p$ and $4s$ levels gives rise to very weak peaks at 54 and 88 eV respectively
- the most intense peak at ca. 335 eV is due to emission from the $3d$ levels of the Pd atoms, whilst the $3p$ and $3s$ levels give rise to the peaks at ca. 534/561 eV and 673 eV respectively.
- the remaining peak is not an XPS peak at all ! - it is an Auger peak arising from x-ray induced Auger emission. It occurs at a kinetic energy of ca. 330 eV (in this case it is really meaningless to refer to an associated binding energy).

Ref: <http://www.chem.qmw.ac.uk/surfaces/scc/>

Inelastic Mean Free Path

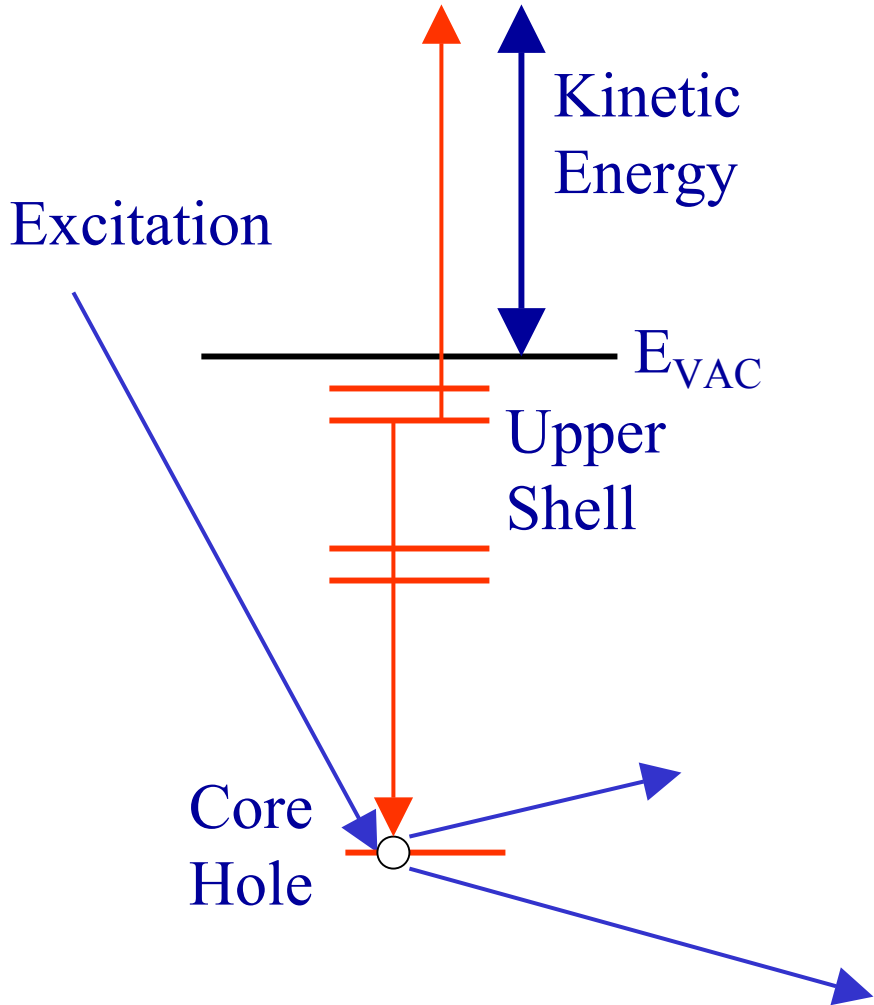


- The IMFP, Λ , follows the “universal curve” in most materials.
- This means that only the surface layers are probed.
- Beer’s law can be used to extract layer thicknesses in heterogeneous thin film structures.



Ref: <http://www.chem.qmw.ac.uk/surfaces/scc/>

Auger Electron Spectroscopy

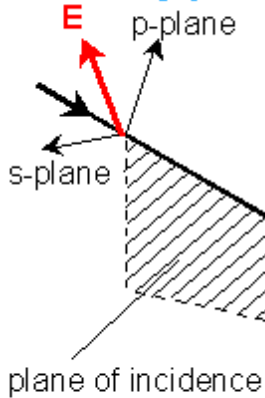


- The nonradiative decay of the ion in a highly excited state may occur via the Auger process.
- The process is independent of the excitation that produces the core hole, so an electron gun may be used as the excitation.
- Auger electrons have characteristic kinetic energies for each element.

VASE

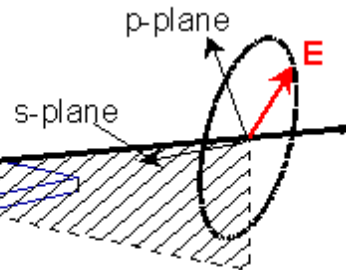
J. A. Woollam Co., Inc

1. linearly polarized light ...



3. elliptically polarized light !

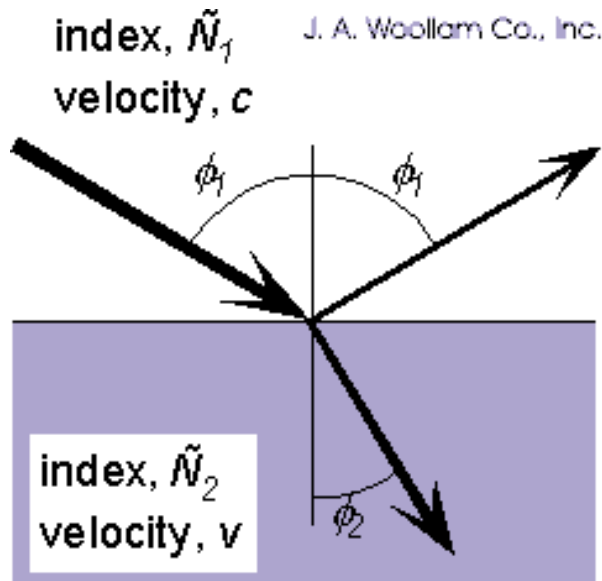
2. reflect off sample ...



$$\rho = \tan(\psi)e^{i\Delta} = \frac{\tilde{R}_p}{\tilde{R}_s}$$

Ellipsometry measures two values, Psi and Delta, that describe the polarization change upon reflection. These values are related to the ratio of Fresnel reflection coefficients, R_p and R_s for p- and s-polarized light, respectively.

Index of Refraction



➤ Reflection

$$\phi_i = \phi_r$$

➤ Refraction (Snell's Law)

- for dielectrics, i.e., $k = 0$

$$n_1 \sin \phi_1 = n_2 \sin \phi_2$$

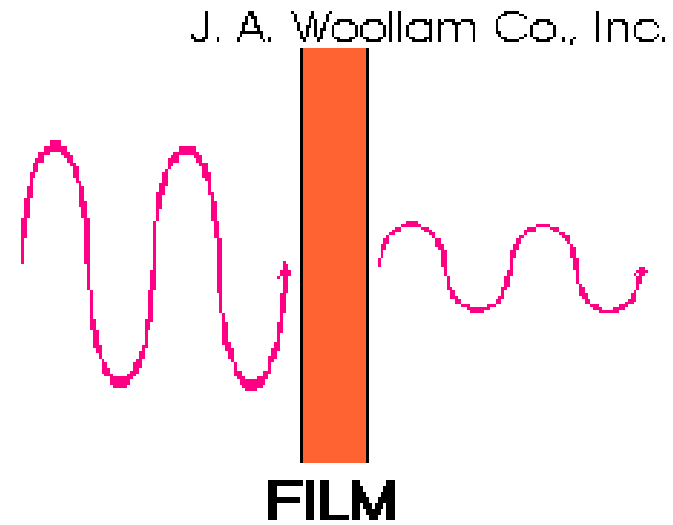
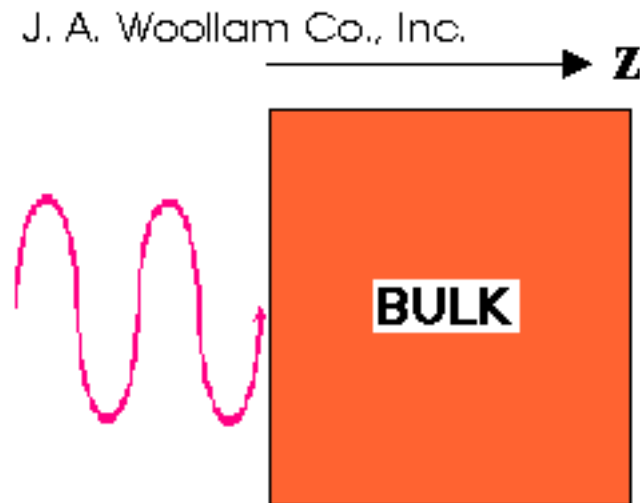
- in general

$$\tilde{N}_1 \sin \phi_1 = \tilde{N}_2 \sin \phi_2$$

Complex Index of Refraction

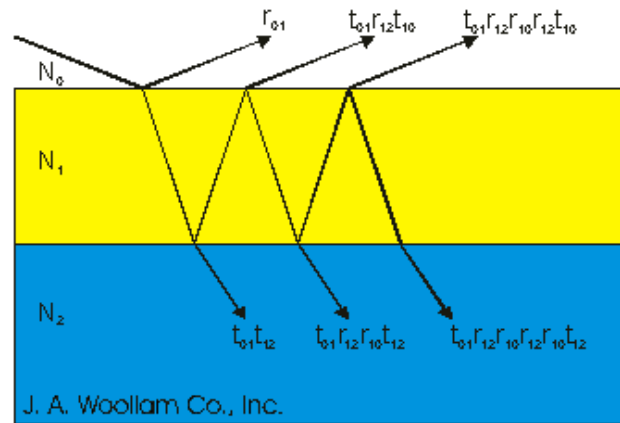
$$\tilde{n}(l) = n(\lambda) + ik(\lambda)$$

$$I = I_0 e^{-\alpha z} \quad \alpha = \frac{4\pi k}{\lambda}$$



Fresnel Coefficients

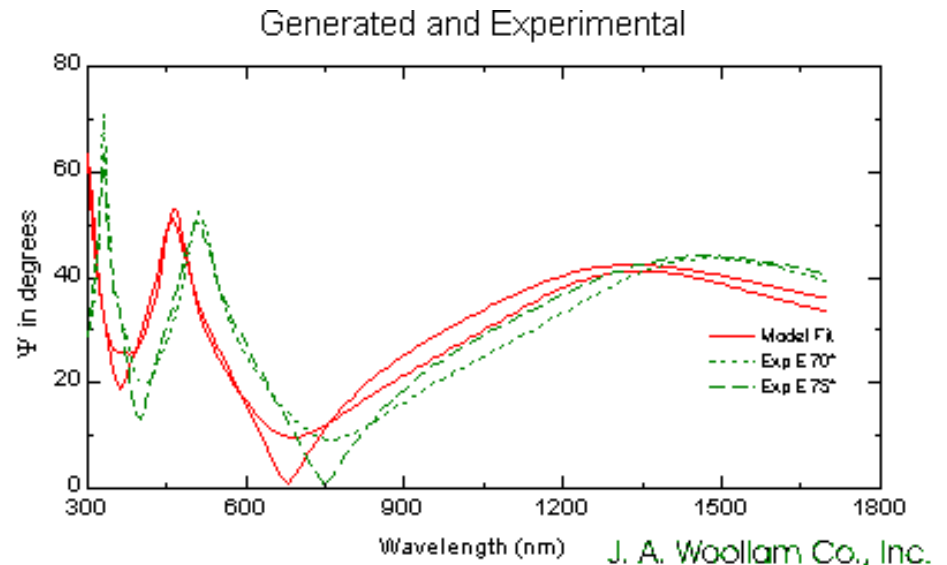
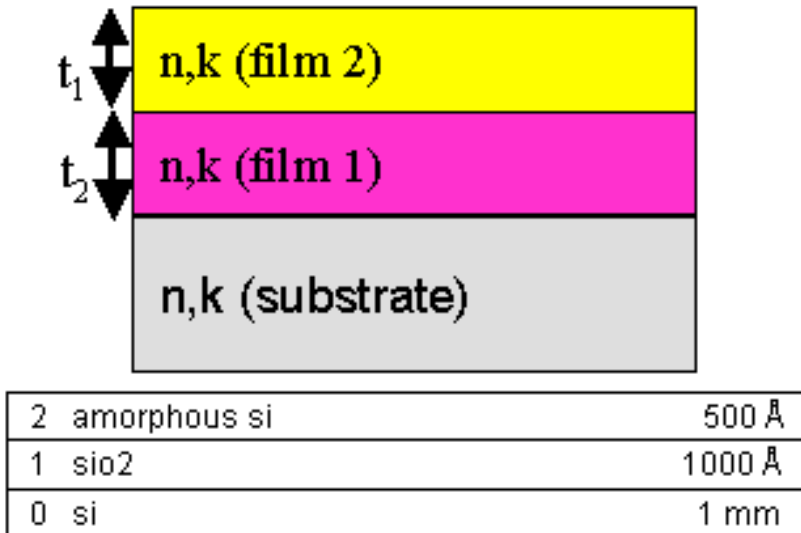
$$\beta = 2\pi \left(\frac{d_1}{\lambda} \right) n_1 \cos \theta_1$$



$$r_{tot} = r_{01} + t_{01}r_{12}t_{10}e^{-2i\beta} + t_{01}r_{12}^2r_{10}t_{10}e^{-4i\beta} + \dots$$

$$R^p = \frac{r_{01}^p + r_{12}^p \exp(-i2\beta)}{1 + r_{01}^p r_{12}^p \exp(-i2\beta)} \quad R^s = \frac{r_{01}^s + r_{12}^s \exp(-i2\beta)}{1 + r_{01}^s r_{12}^s \exp(-i2\beta)}$$

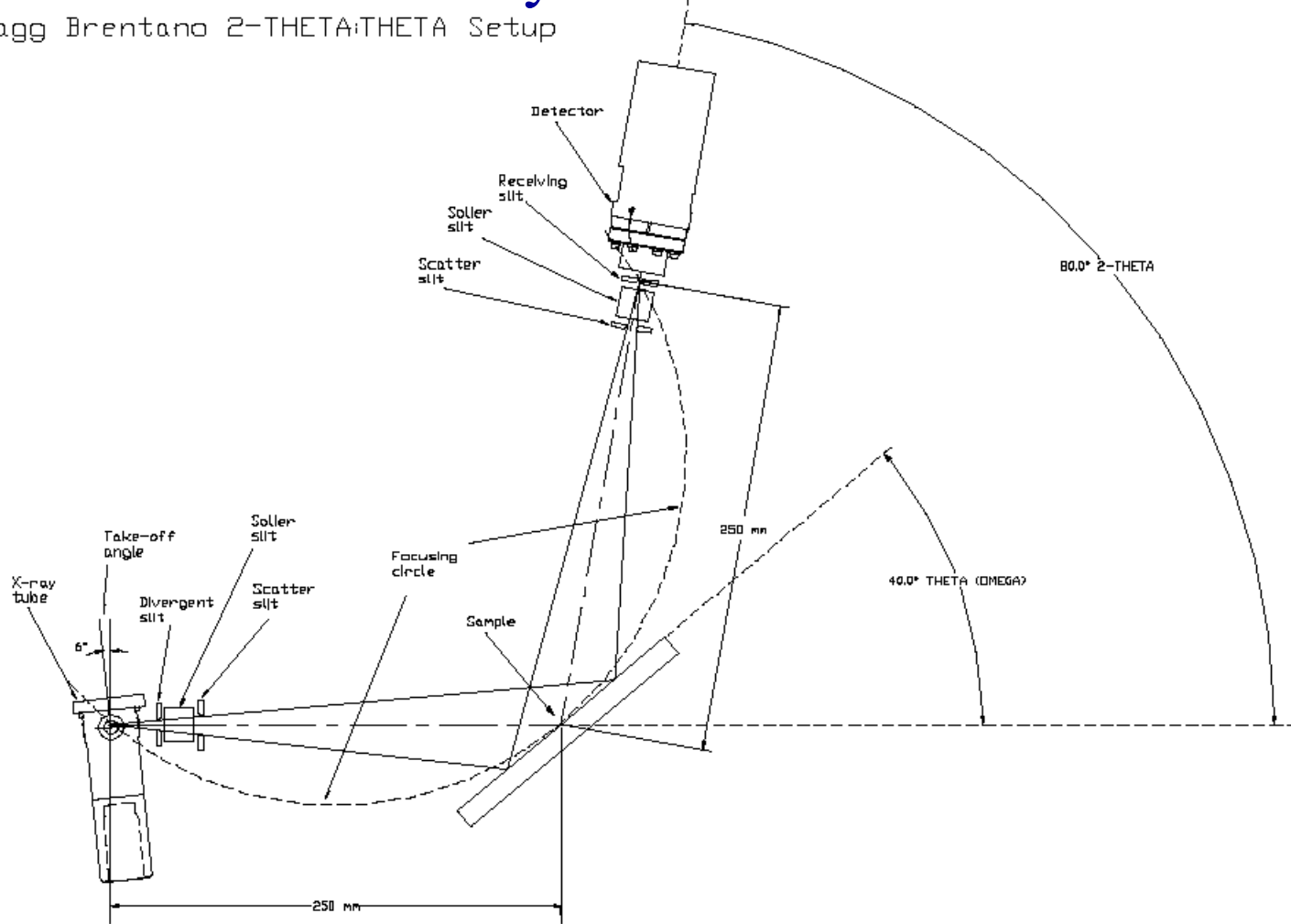
Data and Model



Angle and wavelength dependent data of Ψ & Δ are fitted with the thickness of individual layers as fit parameters—usually the n and k of the bulk film materials must be known before hand.

X-Ray Diffraction

Bragg Brentano 2-THETA:THETA Setup

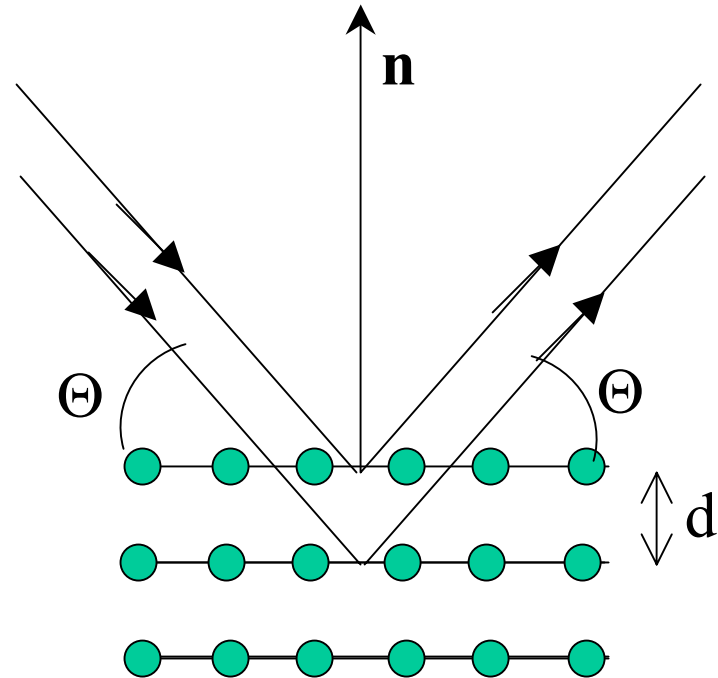


Bragg Diffraction

- The Bragg equation states that constructive interference occurs when the path length difference associated with reflections from adjacent crystal planes is an integral number of wavelengths:

$$2d \sin \Theta = n\lambda$$

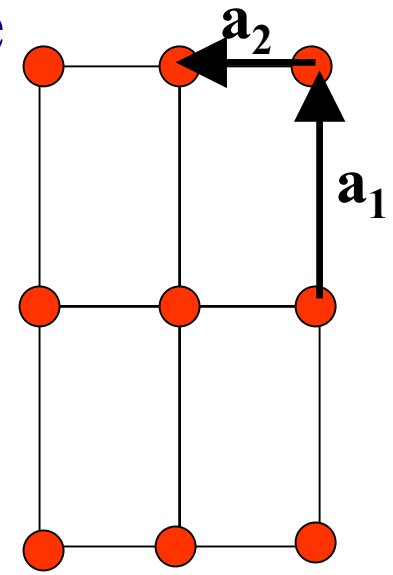
- This basic equation is the starting point for understanding crystal diffraction of x-rays, electrons, neutrons and any other particle which has a DeBroglie wavelength less than an interatomic spacing.



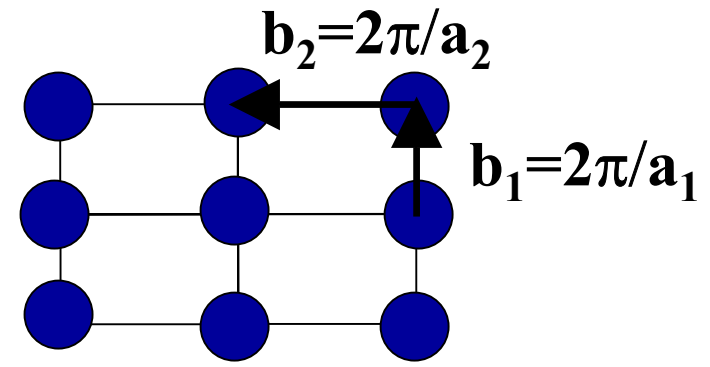
Reciprocal Space

- A Bravais lattice is an infinite array of discrete points with an arrangement and orientation which appears exactly the same, from whichever of the points the array is viewed.
- There are 14 Bravais lattices with primitive vectors a_1 , a_2 , and a_3 .
- The set of all wave vectors k that yield plane waves with the periodicity of a given Bravais lattice is known as the reciprocal lattice.
- The primitive vectors of the reciprocal lattice are found from:

$$\vec{b}_i = 2\pi \frac{\vec{a}_j \times \vec{a}_k}{\vec{a}_i \cdot (\vec{a}_j \times \vec{a}_k)}$$
- Where cyclic permutations of i , j , and k generate the three primitive vector components.



REAL

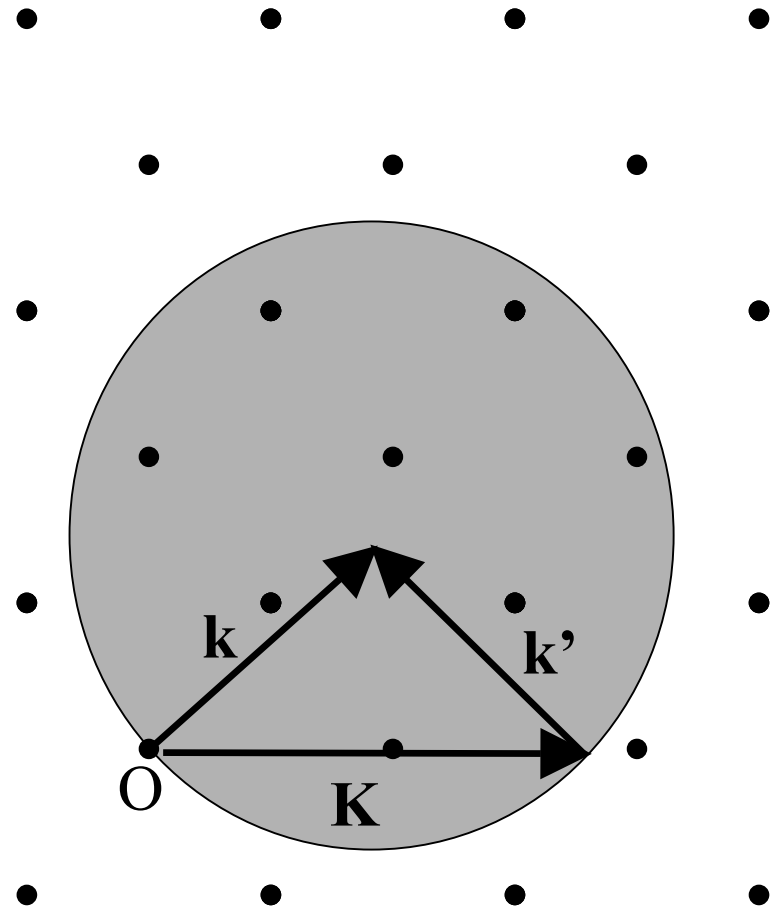


RECIPROCAL

Ref: Ashcroft and Mermin, Solid State Physics (1976).

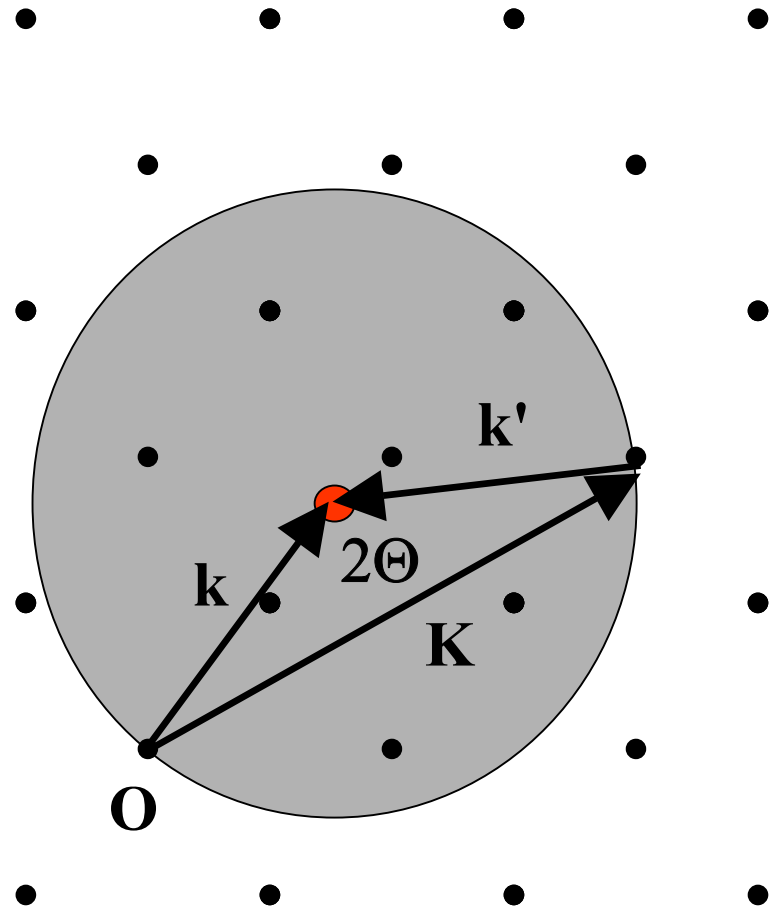
The Ewald Construction

- The Ewald construction is a way to visualize the Laue condition that the change in wavevector is a vector of the reciprocal lattice -- $\mathbf{K} = \mathbf{k}' - \mathbf{k}$, where $k = 2\pi/\lambda$ is the magnitude of the incident wavevector.
- A sphere of radius k is drawn such that its surface intersects a point in reciprocal space and its origin is at the tip of the incident wavevector.
- Any points in reciprocal space which intersect the surface of the sphere indicate where diffraction peaks will be observed *if the structure factor is nonzero*.
- In this example, only the origin intersects the sphere, so there will be no diffraction peaks.



Laue Condition Satisfied

- In this case, the incident wavevector angle is adjusted such that two points lie on the surface of the sphere.
- The diffraction angle is then half the angle between the incident and diffracted wavevectors.
- Generally, only a few angles will yield the proper conditions for diffraction.



Geometrical Structure Factor

- There is a phase associated with diffraction of x-rays from individual atoms and the net ray scattered by a primitive cell is the sum of the individual rays:

$$S_{\mathbf{K}} = \sum_{j=1}^n e^{i\mathbf{K} \cdot \mathbf{d}_j}$$

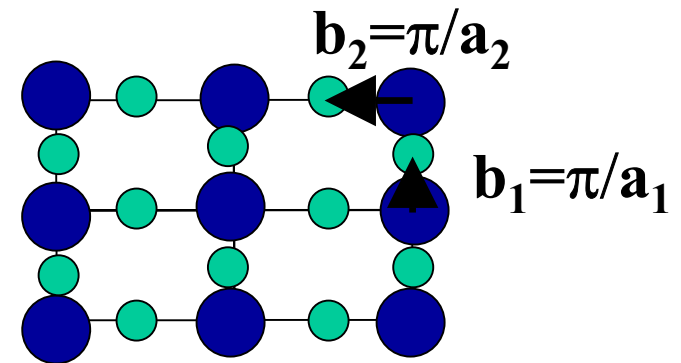
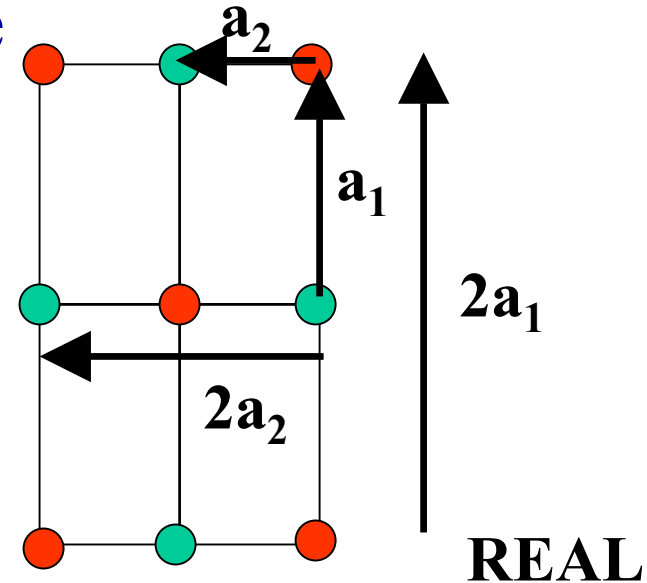
- So even if the Laue condition is met, the structure factor may be zero and no diffraction peak will be observed.
- An example is the bcc lattice where the sum of the indices of the reciprocal lattice vectors must be even for the structure factor to be nonzero. If the sum of the indices is odd, then no peak will be observed.
- For a polyatomic lattice this is replaced by the atomic form factor....

Reciprocal Space

- Doubling the periodicity in real space produces twice as many diffraction spots in reciprocal space.
- This effect can be produced chemically with an ordered binary alloy.
- The primitive vectors of the reciprocal lattice are found from:

$$\vec{b}_i = 2\pi \frac{\vec{a}_j \times \vec{a}_k}{\vec{a}_i \cdot (\vec{a}_j \times \vec{a}_k)}$$

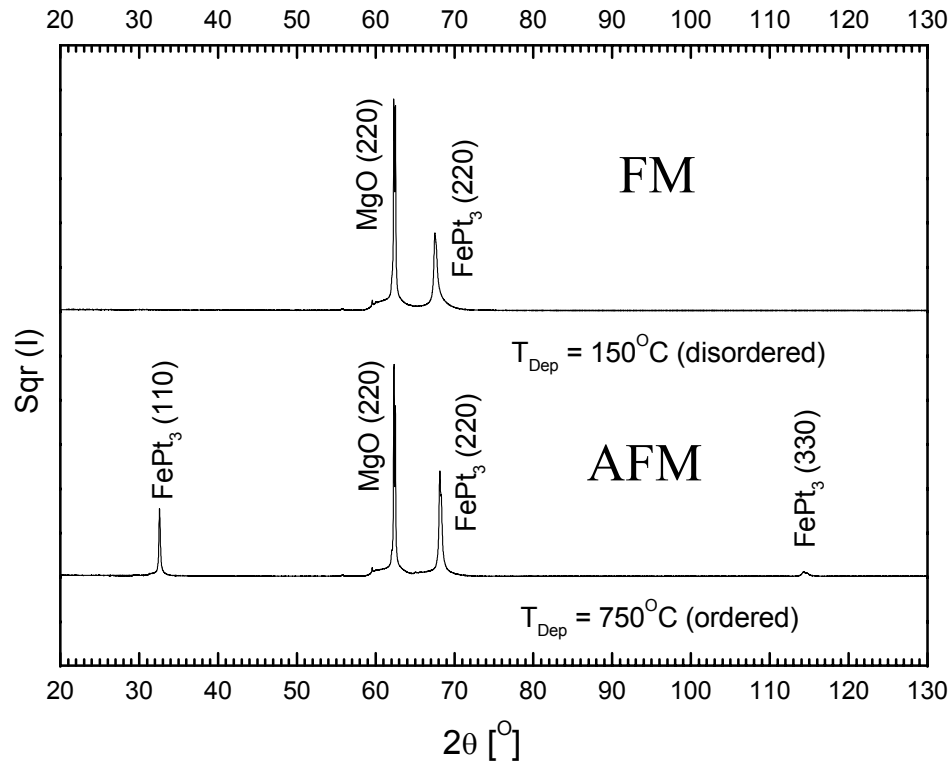
- A doubling of the periodicity in real space will produce half-order spots in reciprocal space..



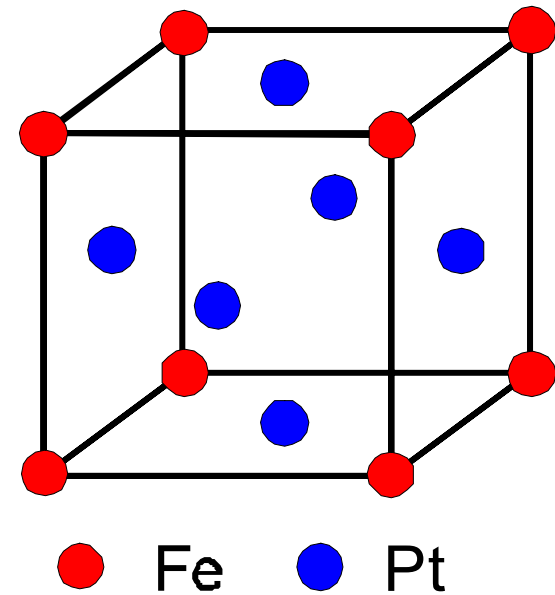
Ref: Ashcroft and Mermin, Solid State Physics (1976).

RECIPROCAL

Growth of Epitaxial FePt₃ on MgO



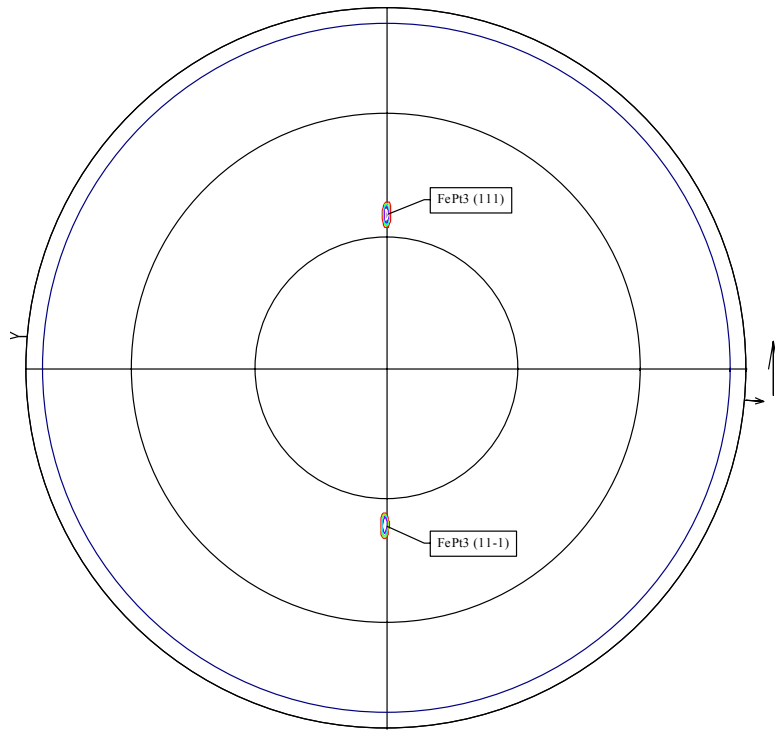
Out of plane XRD



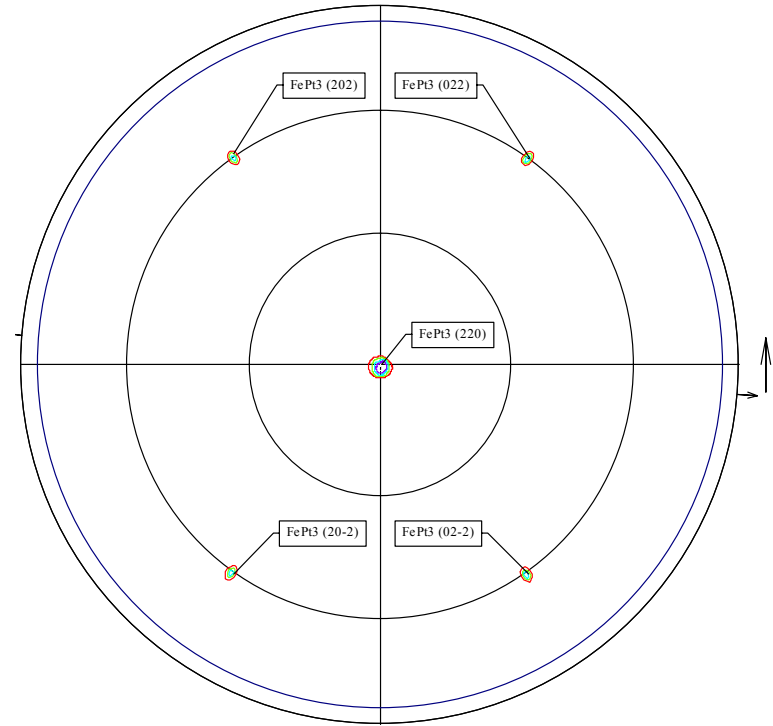
L₁₂ structure

Ref. S. Maat, et al., PRB (2001).

Pole Figures FePt₃ Ordered Phase



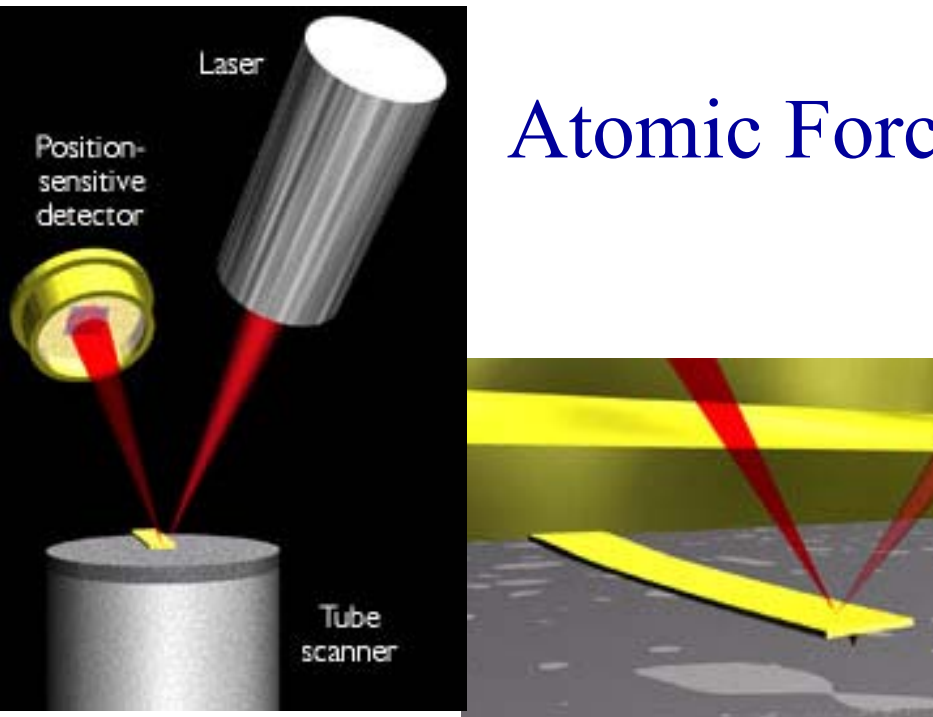
$\langle 111 \rangle$ planes



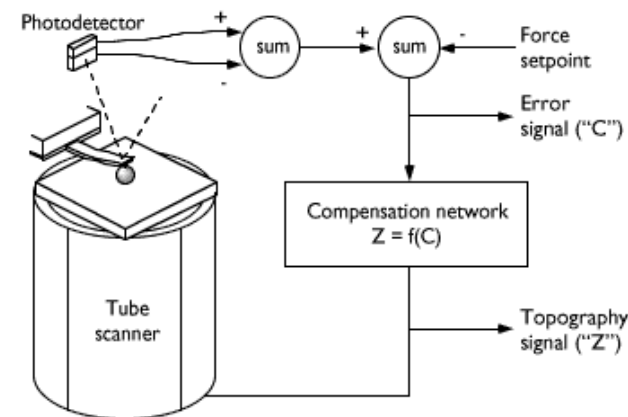
$\langle 220 \rangle$ planes

Ref. S. Maat, et al., PRB (2001).

Atomic Force Microscopy

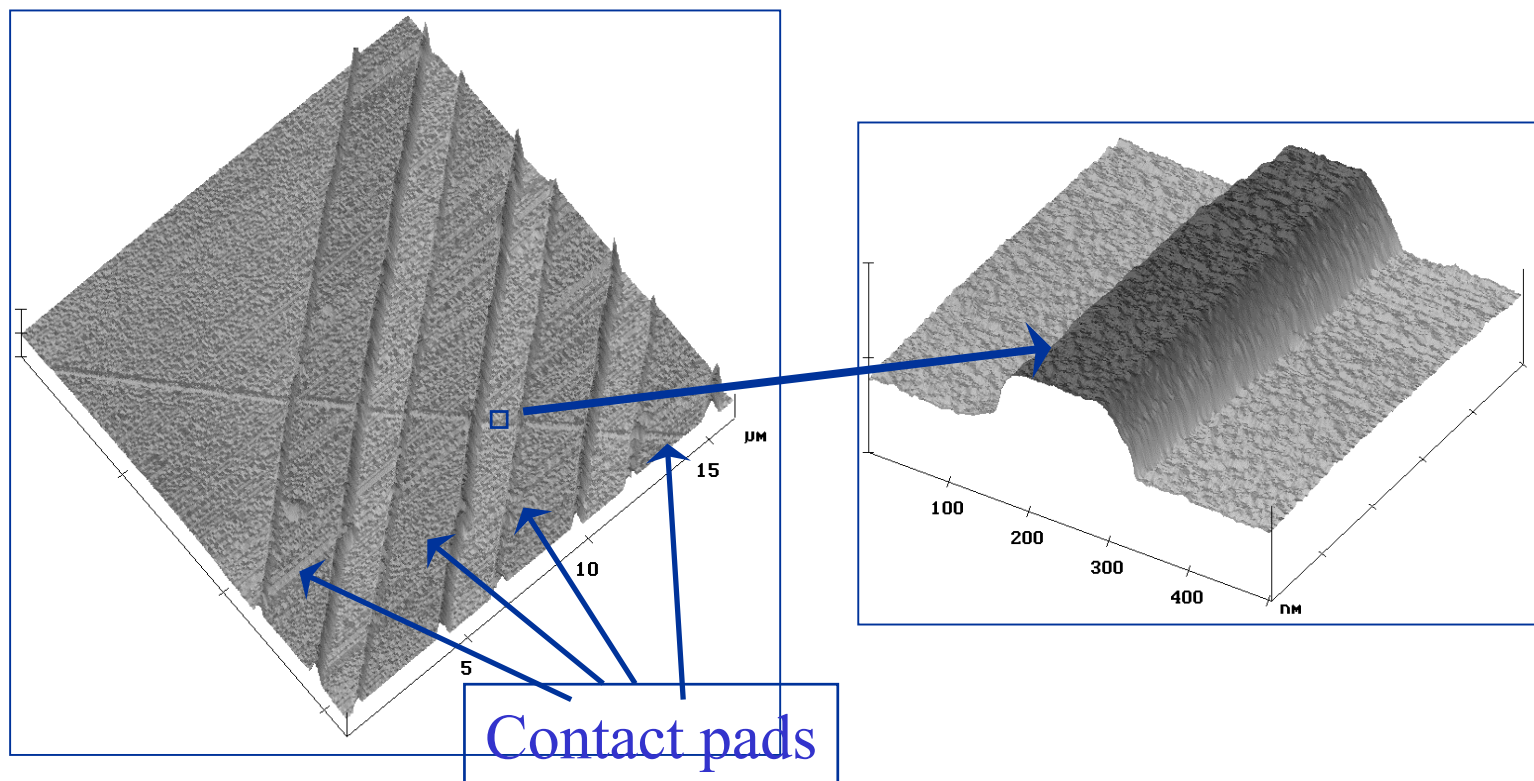


- A cantilever with a tiny tip on its end is scanned across a surface while maintain a constant feedback signal proportional to the interaction between the probe tip and surface.
- The minimum force that can be detected is 100 pn.
- The tip has a nominal radius of >10 nm which limits the spatial resolution.
- The tip exerts a measuring pressure of about 1 MPa or 10 atmospheres on the surface being measured.



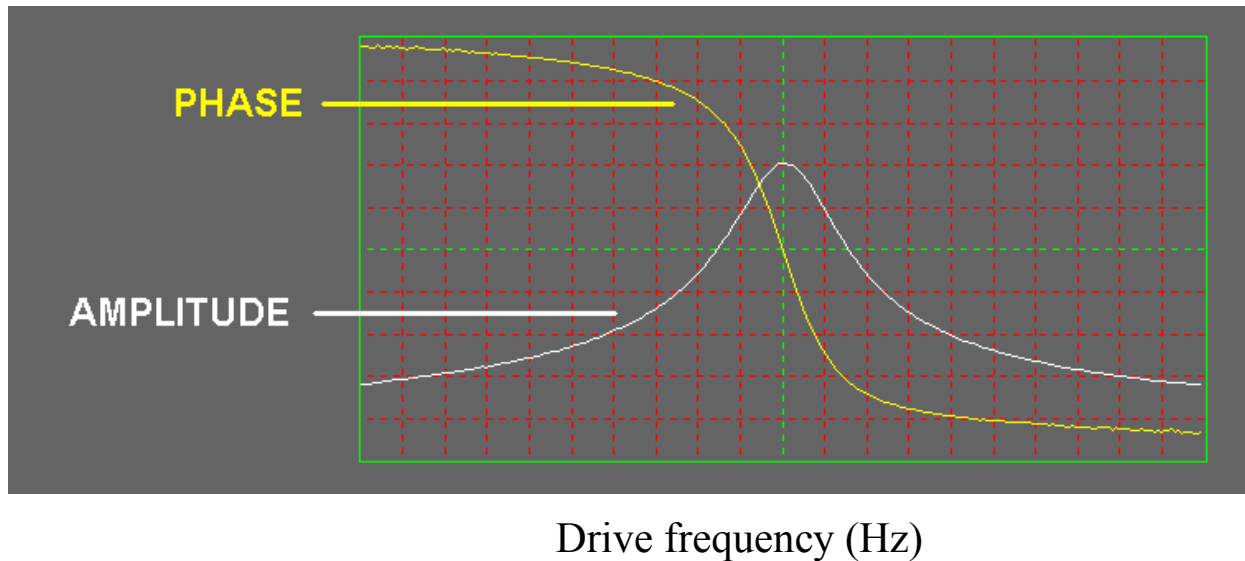
<http://stm2.nrl.navy.mil/how-afm/how-afm.html>

AFM Images of a 150-nm Permalloy Wire Fabricated by Phase Mask Lithography



Ref. H. Jiang, et al., MRS Spring Meeting (1999).

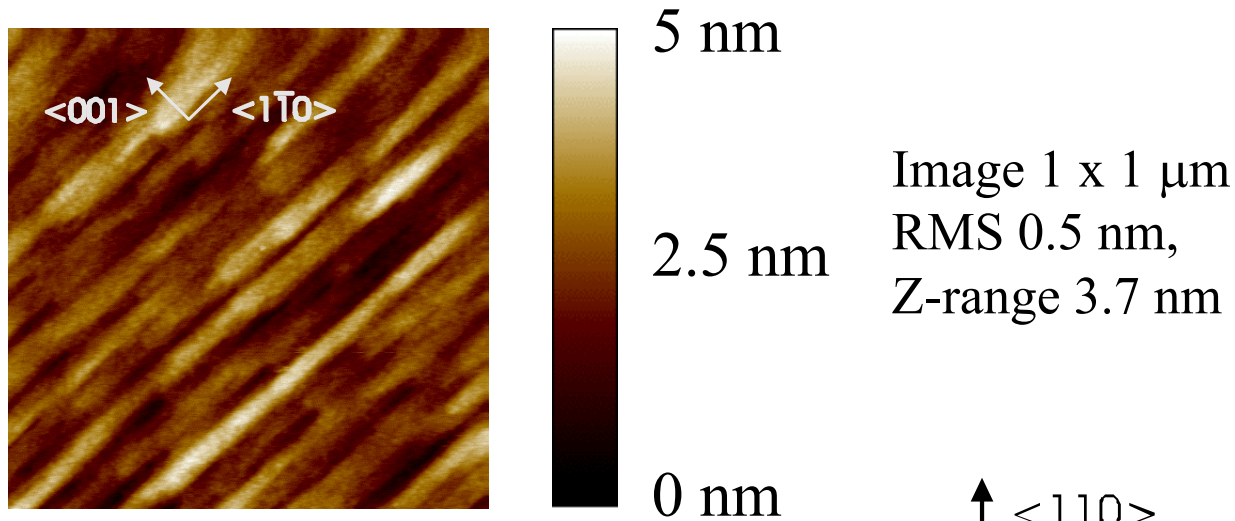
Tapping Mode



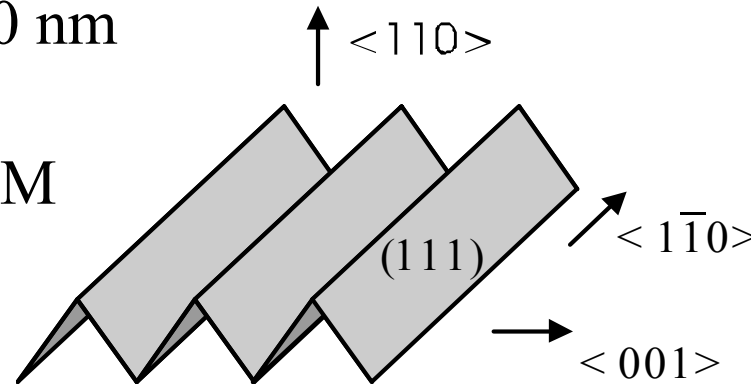
- The cantilever is vibrated at its resonant frequency by a tiny piezoelectric element in the tip holder.
- The z-position of the tip is adjusted to keep the vibration amplitude constant.
- This mode has increased signal to noise ratio and it avoids the tip sticking to the surface.

<http://stm2.nrl.navy.mil/how-afm/how-afm.html>

AFM of FePt₃ on MgO(110)



(111) facets are visible in AFM



Ref. S. Maat, et al., PRB (2001).

MFM

Driven Harmonic Oscillator

$$m \ddot{z} + c \dot{z} + Kz = F_0 e^{i\omega t}$$

Assume $z = A e^{i(\omega t - \phi)}$

Then $A(K - m\omega^2) = F_0 \cos \phi$
 $A\omega c = F_0 \sin \phi$

so $\tan \phi = \frac{c\omega}{K - m\omega^2}$
 $A = \frac{F_0}{\sqrt{(K - m\omega^2)^2 + c^2\omega^2}}$

Define $\omega_0 \equiv \sqrt{K/m}$ $\gamma \equiv c/m$

$\therefore \tan \phi = \frac{\gamma\omega}{\omega_0^2 - \omega^2}$
 $A = \frac{F_0/m}{\sqrt{(\omega_0^2 - \omega^2)^2 + \gamma^2\omega^2}}$

Now lets add a force
 $F_{\text{mag}} = f(z - z_{\text{tip}}) = f z - f z_{\text{tip}}$

adding a constant force to the above equation does not change the amplitude, A, or phase, ϕ , so we assume to first order. $F_{\text{mag}} = f z$.

Then we get

$$m \ddot{z} + c \dot{z} + (f + K)z = F_0 e^{i\omega t}$$

Just replace K with $f + K$ in the above equations. Then:

$$\tan \phi = \frac{c\omega}{f + K - m\omega^2} = \frac{\gamma\omega}{f + (\omega_0^2 - \omega^2)}$$

$$A = \frac{F_0/m}{\sqrt{(f + K - m\omega^2)^2 + c^2\omega^2}}$$

We measure $\phi = \frac{\pi}{2} + \phi_{\text{mag}}$

Use:

$$\tan(\alpha + \beta) = \frac{\tan \alpha + \tan \beta}{1 + \tan \alpha \tan \beta} \quad \text{and take}$$

the limit as $\alpha \rightarrow \pi/2$.

$$\lim_{\alpha \rightarrow \pi/2} \frac{\tan \alpha + \tan \beta}{1 + \tan \alpha \tan \beta} = \frac{\sec^2 \alpha}{\tan \beta \sec^2 \alpha} = \frac{1}{\tan \beta}$$

So:

$$\tan \phi = \frac{1}{\tan \phi_{\text{mag}}} = \frac{\gamma\omega}{f + (\omega_0^2 - \omega^2)}$$

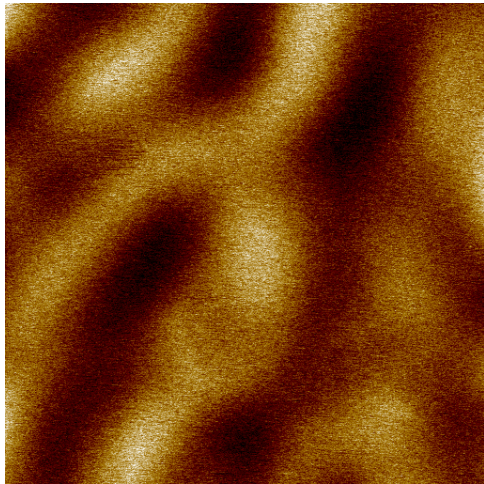
$$\omega_0^2 - \omega^2 \approx 0 \quad \text{so} \quad \tan \phi_{\text{mag}} = \frac{\gamma\omega}{f}$$

$$\phi_{\text{mag}} \text{ is small so } \tan \phi_{\text{mag}} \approx \phi_{\text{mag}} = \frac{f}{\gamma\omega}$$

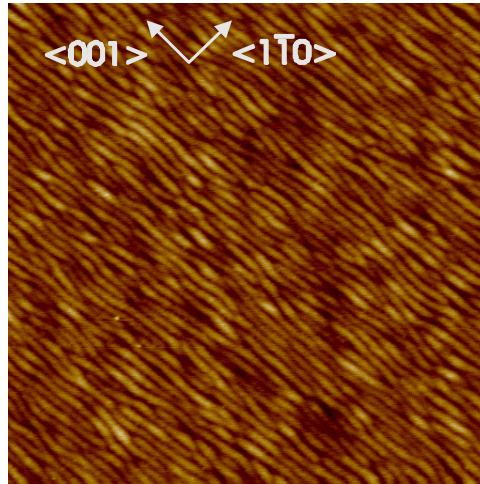
$$\therefore \phi_{\text{mag}} \propto f = dF_{\text{mag}}/dz$$

- For MFM the phase of the vibrating cantilever held above the surface is proportional to the z-derivative of the magnetic force.

FePt₃ on MgO (110)



MFM



AFM

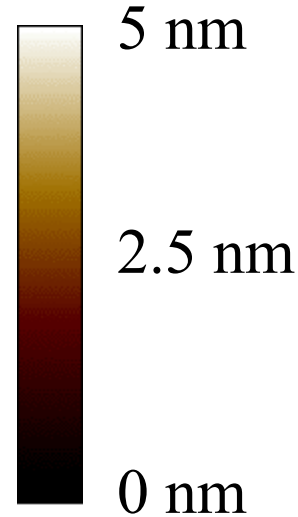
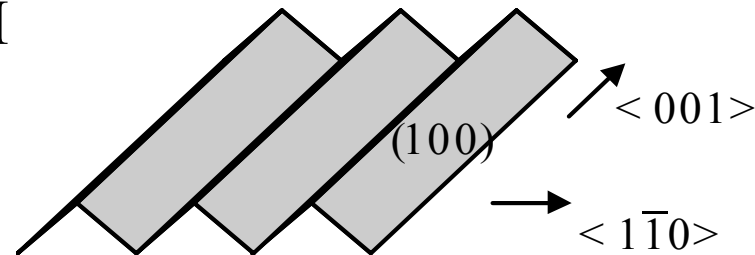


Image 1 x 1 μm
RMS 0.7 nm,
Z-range 4.5 nm

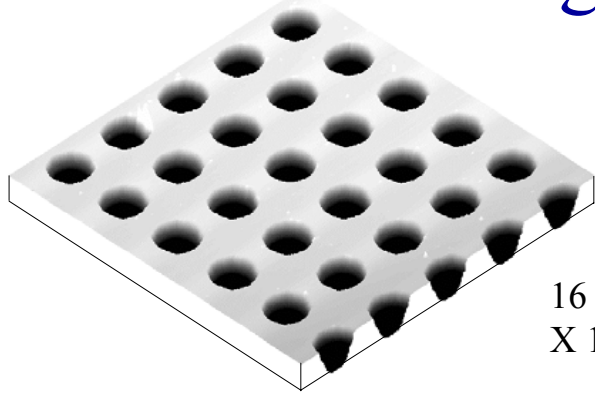
↑ <110>

(100) facets are visible in AFM
typical domain size ~ 250 nm

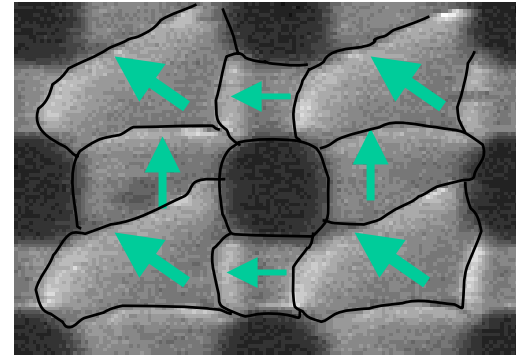


Ref. S. Maat, et al., PRB (2001).

Ferromagnetic Antidot Arrays

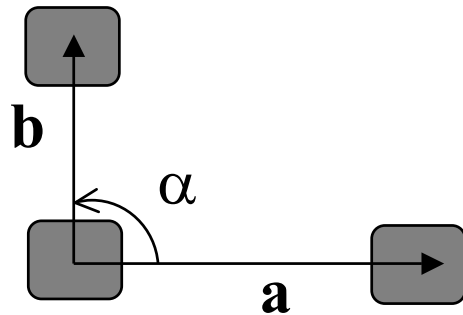


16 micrometer
X 16 micrometer



Close up

2-D hole array (antidot)



Antidot unit mesh

Domain pinning at hole edges
with MFM

Ref. C. Yu, J. Appl. Phys. (1999).

Liouville's Theorem

- The phase space volume occupied by a collection of systems evolving according to Hamilton's equation of motion will be preserved in time.
- The cost of increased resolution (better information) is reduced counting rate (lower signal to noise) and a subsequent increased acquisition time if the sensitivity of the apparatus remains unchanged.
- Match the instrument to the quality information you want.



$$\dot{q}_i = \frac{\partial H}{\partial p_i}$$

$$\dot{p}_i = -\frac{\partial H}{\partial q_i}$$

$$\dot{H} = -\frac{\partial L}{\partial t}$$

$$L = T - V$$